JCTC Journal of Chemical Theory and Computation

Article

pubs.acs.org/JCTC

Noncovalent Interactions of DNA Bases with Naphthalene and Graphene

Yeonchoo Cho,[†] Seung Kyu Min,[†,∥] Jeonghun Yun,[†] Woo Youn Kim,[‡] Alexandre Tkatchenko,[§] and Kwang S. Kim*,[†]

[†]Center for Superfunctional Materials, Department of Chemistry, Pohang University of Science and Technology, San 31, Hyojadong, Namgu, Pohang 790-784, Korea

[‡]Department of Chemistry and KAIST Institute for NanoCentury, KAIST, Daejeon 305-701, Korea

[§]Fritz-Haber-Institut der Max-Planck-Gesellschaft, Faradayweg 4-6, 14195, Berlin, Germany

ABSTRACT: The complexes of a DNA base bound to graphitic systems are studied. Considering naphthalene as the simplest graphitic system, DNA base−naphthalene complexes are scrutinized at high levels of ab initio theory including coupled cluster theory with singles, doubles, and perturbative triples excitations [CCSD(T)] at the complete basis set (CBS) limit. The stacked configurations are the most stable, where the CCSD(T)/CBS binding energies of guanine, adenine, thymine, and cytosine are 9.31, 8.48, 8.53, 7.30 kcal/mol, respectively. The energy components are investigated using symmetry-adapted perturbation theory based on density functional theory including the dispersion energy. We compared the CCSD(T)/CBS results with several density functional methods applicable to periodic systems. Considering accuracy and availability, the optB86b nonlocal functional and the Tkatchenko−Scheffler functional are used to study the binding energies of nucleobases on graphene. The predicted values are 18−24 kcal/mol, though many-body effects on screening and energy need to be further considered.

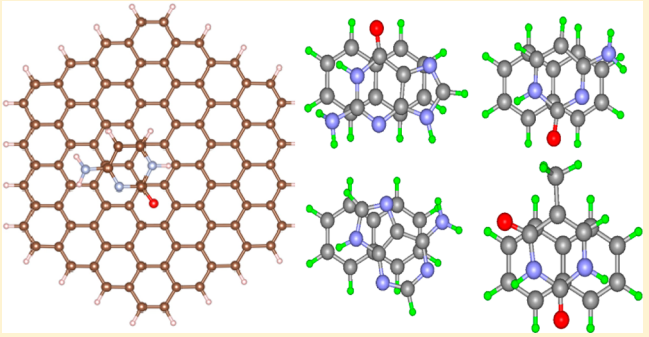

1. INTRODUCTION

The π-interactions[1−3] play a crucial role in self-assembling[4−6] and nanorecognition.[7−10] Numerous calculations were carried out to accurately describe π-interactions,[11−15] in particular, $\pi-\pi$ interactions.[16−24] Here we are particularly interested in the recognition of nucleobases using π-stacking interactions.[25−27] To this end, graphene is a good candidate because of its π-conjugated structure and sensitivity to perturbation. As graphene has intriguing physical and chemical properties,[28,29] it led to a burst of researches in recent years.[30−36] One of interesting applications of graphene is a biosensor where carbon-based materials are employed.[37] We recently proposed a fast DNA sequencing method utilizing strong $\pi-\pi$ stacking between graphene and nucleobase.[38,39] In this case, the binding energy needs to be strong enough to hold nucleobases on graphene and reduce noises in measurement and weak enough to translocate a single-stranded DNA over graphene nanoribbon in a nanochannel.

Several theoretical studies on the interaction between nucleobases and graphene have been reported, partly thanks to the remarkable improvement of recent van der Waals (vdW) methods. Optimization from density functional theory (DFT) using local density approximation by Gowtham et al. shows that all the nucleobases are separated from a graphene sheet by about 3.5 Å and binding is strongest for guanine (14 kcal/mol), while it is similar for other nucleobases (11 kcal/mol).[40] They also showed that translocation parallel to the graphene surface has a low barrier, maximally 2.3 kcal/mol. Antony et al. used B97-D functional to optimize the same systems.[41] They expected significantly closer base−graphene distances as low as 3.0 Å. Another recent study by Berland et al.[42] using Dion's nonlocal functional[43] predicts, for an adenine molecule, the adsorption energy of 16.4 kcal/mol at an equilibrium separation of 3.5 Å.[42] Most recently, Le et al. used newly developed DFT vdW methods to compute binding energies.[44] Free energy calculations are also made to show that graphene−nucleobase binding is favored even in solution.[45] Overall, at the current stage the binding energy and distance between nucleobase and graphene are not clearly resolved.

Here, we apply state-of-art wave function theories as well as density functional methods to obtain reliable results for interactions between graphene and nucleobases. We compute binding characteristics of nucleobases on naphthalene and graphene. The π stacking interaction is a traditionally difficult problem at which most DFT methods are poor and even some of high-level quantum chemical methods show a poor performance.[1,17] However, extended systems can only be dealt with DFT methods. Thus, we begin from nucleobase−naphthalene complexes where most of quantum chemical

Received: December 14, 2012
Published: March 5, 2013

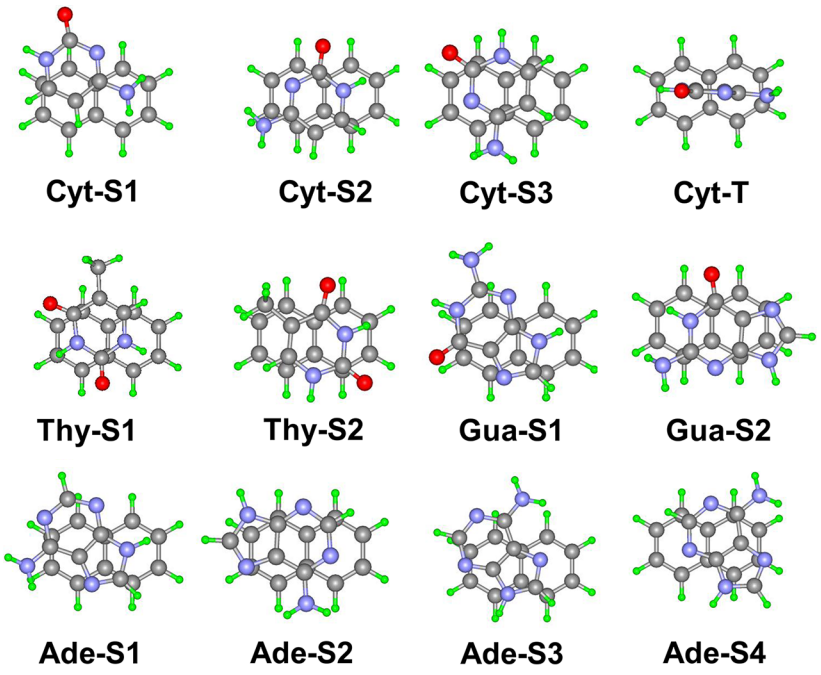

Figure 1. Optimized geometries of nucleobase−naphthalene complexes at the MP2/aVDZ level. Gray, green, blue, and red are carbon, hydrogen, nitrogen, and oxygen, respectively.

methods are applicable. High-level computations up to the coupled cluster level are reported. Symmetry-adapted perturbation theory (SAPT)[46] is applied to analyze binding characteristics. We also apply DFT with optB86b,[47] vdW-DF2[48] functional, and Tkatchenko−Scheffler functional[49] (TS), both of which have recently developed to evaluate vdW interactions. Then, these are applied to extended systems where a nucleobase is adhered onto graphene. We excluded hybrid functionals because required memory is too large to compute a single molecule on a surface.

2. METHODS

We first examine geometry and energetics of naphthalene−nucleobase model systems. We apply a basin-hopping procedure with the dispersion-augmented density functional tight-binding method.[50] This process allows us to efficiently reduce the number of configurations under consideration. The low-energy configurations are further optimized with the second-order Moller−Plesset perturbation theory (MP2) using the aug-cc-pVDZ (aVDZ) basis set.[17] We again narrow our focus to low-energy configurations at the MP2/aVDZ level.

Starting from these geometries, we optimize the vertical distance and obtain the binding energy with several theories to find out which method most accurately describes the system. The reference is coupled cluster theory with single, double, and perturbative triple excitations (CCSD(T)) at the complete basis set (CBS) limit. The CBS limit at the CCSD(T) level is estimated from the CBS correction to the RIMP2/aVDZ level according to the following equation:[51,52]

$$E^{\mathrm{CCSD(T)/CBS}} = E^{\mathrm{CCSD(T)/aVDZ}} + \frac{3^3 E^{\mathrm{MP2/aVTZ}} - 2^3 E^{\mathrm{MP2/aVDZ}}}{3^3 - 2^3} - E^{\mathrm{MP2/aVDZ}}$$

The distance is estimated from coupled cluster theory with single and double excitations (CCSD) with the aVDZ basis set.[53] The spin-component scaled MP2 (SCS-MP2)[54] is also applied with the aug-cc-pVTZ (aVTZ) basis set.[17] All the Hartree−Fock based correlation methods are done under the resolution-of-identity approximation and the frozen core approximation. The basis set superposition error is corrected using the counterpoise method.

Moreover, we included DFT schemes that show remarkable performances on vdW interactions. The asymptotically corrected[55] DF-SAPT(DFT)[46] with the PBE0 functional[56] is employed to analyze binding characteristics. Grimme's dispersion correction schemes are employed with aVTZ basis: B97-D and BLYP-D3.[57] B97-D is B97 reparameterized in the presence of DFT-D2 dispersion correction. DFT-D3 in BLYP-D3 is an improvement from DFT-D2 in that atomic C_6 coefficients depend on the so-called coordination numbers and $1/R^8$ terms are included. We also examine the effect of including three-body terms. Grimme et al. developed the Axilrod−Teller−Muto type correction to D3 scheme, but this correction is excluded in the default setting partly because reference data for large systems are limited. The OptB86b[47] and vdW-DF2[48] nonlocal functional implemented in VASP[58] is used with cutoff 600 eV. They correct any inaccuracy of the original vdW-DF, approximated from the adiabatic connection fluctuation dissipation (ACFD) correlation, mainly by employing different exchange enhancement factors in generalized gradient approximation. Thanks to algorithmic advances by Roman-Perez and Soler,[59] a nonlocal correction is computed in a shorter time than the KS energy. The TS scheme[49] uses Hirshfeld volumes to compute environment dependency of dispersion interaction coefficients, in contrast to Grimme's DFT-D2 where dispersion coefficients are fixed. We used the tier 2 basis of the tight setting implemented in FHI-AIMS.[60] We also applied the many-body dispersion (MBD) scheme by Tkatchenko and Scheffler.[61] They introduce the coupled fluctuating dipole Hamiltonian to take into account screening

and the effects beyond pairwise additivity. These methods are less costly than MP2 and can be applied to extended structures. Therefore, we compute the binding energy between graphene and nucleobases. The unit cell (and the graphene sheet) is chosen to be large so that the closest atom in a nearest neighbor cell is at least 5.5 Å away. This minimizes spurious interactions between neighboring cells.

3. RESULTS AND DISCUSSIONS

Figure 1 shows low-energy configurations. Table 1 lists the vertical distances (r_v) and binding energies at the MP2 level.

Table 1. BSSE-Corrected Binding Energies (kcal/mol) and CBS Limits (kcal/mol) Estimated From Vertical Distances (r_v/Å) Optimized at the MP2/aVTZ Level[a]

	Cyt-S1	Cyt-S2	Cyt-S3	Cyt-T
aVDZ	9.94	10.43	9.63	6.97
aVTZ	10.66	11.25	10.52	7.49
CBS	10.96	11.59	10.89	7.70
r_v	2.95	2.93	3.05	3.21
	Thy-S1	Thy-S2	Gua-S1	Gua-S2
aVDZ	11.22	12.35	12.57	13.46
aVTZ	12.28	11.81	13.67	14.56
CBS	12.73	11.59	14.13	15.02
r_v	2.90	3.00	2.93	2.94
	Ade-S1	Ade-S2	Ade-S3	Ade-S4
aVDZ	12.93	10.85	11.20	10.43
aVTZ	13.85	11.75	12.11	11.31
CBS	14.23	12.12	12.49	11.67
r_v	2.91	3.03	2.92	3.04

[a]After fully relaxed at the MP2/aVDZ level, only the vertical distance is adjusted at the MP2/aVTZ level. The vertical distance is estimated by the difference between the averaged z coordinate (the z-axis is perpendicular to the naphthalene plane) of naphthalene carbons and the nucleobase ring atom vertically closest to naphthalene.

Not surprisingly, stable configurations are stacked configurations except for the T-shaped one in the cytosine case. However, the T-shaped configuration is less stable than any of stacked configurations. The plane of a nucleobase is slightly tilted to the plane of naphthalene in most cases. We define the vertical distance as the distance from the naphthalene plane to the ring atom of a base closest to that plane. Considering that the base is tilted, the vertical distance is increased by ∼0.1 Å if defined as the averaged distance of ring atoms to the naphthalene plane. Note that the binding energy depends significantly on the basis set size, as is well-known for MP2 methods. There are nearly isoenergetic configurations among the stacked, but their binding characteristics are similar, so we mainly discuss the lowest-energy structure for each nucleobase−naphthalene complex: Cyt-S2, Thy-S1, Gua-S2, and Ade-S1.

Table 2 consists of binding energies and vertical distances at various levels for configurations selected above. We optimized only the vertical distance for clear comparison, while fixing all the other atomic degrees of freedom. We also computed the CCSD(T)/aVDZ binding energy at the CCSD/aVDZ-optimized vertical distance. Assuming that both CCSD(T) and MP2 values of $E_{CBS} - E_{aVDZ}$ are similar, the CCSD(T)/CBS binding energies of Cyt-S2, Thy-S1, Gua-S2, and Ade-S1 are 7.62, 8.53, 9.31, and 8.48 kcal/mol, respectively. Naphthalene binds most strongly with guanine, followed by thymine, adenine, which are comparable, and least strongly with cytosine. This trend is not consistent in every method we employed. All DFT methods employed except for SAPT(DFT) predict that thymine binds strongly than adenine does, although the difference is overestimated. SAPT(DFT) and SCS-MP2 predict the reverse: adenine binds stronger than thymine. We also computed CCSD(F12*)(T**)/aVDZ[62−64] binding energies. The double star on triples means that the triples correlation energy of each single-point calculation is scaled by the ratio of MP2-F12 to MP2 correlation energies for a complex. This choice of the scaling factor (i.e., applying the scaling factor of the complex to all cases) is somewhat arbitrary. One can employ the scaling factor of corresponding single-point calculation, called the (T*) approximation. However, it breaks size consistency, and in any case differences are within 0.2 kcal/mol. CCSD(F12*)(T**)/aVDZ binding energies are expected to be close to the CCSD(T)/aVQZ values. One can observe that CCSD(F12*)(T**)/aVDZ binding energies are between CCSD(T)/aVDZ and CBS numbers.

On the other hand, the distance between nucleobase and naphthalene is similar throughout bases at each level of theory.

Table 2. Method-Dependent BSSE-Corrected Binding Energies (kcal/mol) along with the Optimized Vertical Distances (Å) in Parentheses[a]

$E_b(r_v)$	Cyt-S2	Thy-S1	Gua-S2	Ade-S1
CCSD/aVDZ	5.05(3.33)	5.91(3.35)	6.29(3.35)	5.71(3.33)
CCSD(T)/aVDZ	6.98	7.79	8.65	7.92
CCSD(T)/CBS	7.62	8.53	9.31	8.48
CCSD(F12*)(T**)/aVDZ	7.33	8.38	9.23	8.29
SCS-MP2/aVTZ	7.30(3.19)	8.12(3.22)	9.42(3.19)	9.05(3.16)
optB86b/600	8.65(3.19)	10.29(3.20)	10.87(3.21)	9.53(3.20)
vdW-DF2/600	7.02(3.34)	8.17(3.35)	8.52(3.36)	7.61(3.35)
PBE0 + TS/tier 2	7.86(3.25)	9.66(3.25)	10.16(3.26)	8.83(3.24)
PBE + TS/tier 2	8.16(3.24)	9.76(3.25)	10.45(3.26)	9.18(3.23)
PBE + MBD/tier 2	7.84(3.24)	9.45(3.26)	10.32(3.25)	8.94(3.24)
B97-D/aVTZ	7.22(3.16)	8.83(3.16)	9.48(3.16)	8.39(3.14)
BLYP-D3/aVTZ	8.03(3.18)	9.59(3.19)	9.99(3.21)	8.64(3.20)
BLYP-D3 + $E^{(3)}$/aVTZ	7.72(3.19)	9.24(3.19)	9.60(3.21)	8.30(3.20)
SAPT(PBE0)/aVDZ[a]	7.41(3.23)	8.31(3.26)	9.58(3.25)	8.70(3.23)

[a]Fragment relaxation energies are computed at the same level and added to the SAPT interaction energies.

The difference is within 0.03 Å in all but SCS-MP2. Exceptions are B97-D and vdW-DF2. The former predicts too short, the latter too long. In any case, these differences between bases are negligible since the potential energy surface is flat and the corresponding energy difference is well within the thermal fluctuation range. However, different methods predict distances different up to 0.2 Å.

The characteristics of binding between DNA-bases and naphthalene are investigated with SAPT.[46] Table 3 lists the

Table 3. SAPT(PBE0)/aVDZ Energy Components (kcal/mol) of the Lowest Energy Structures of Nucleobase−Naphthalene Complexes

	Cyt-S2	Thy-S1	Gua-S2	Ade-S1
E_{tot}	−6.80	−7.89	−8.79	−7.84
E_{es}	−4.61	−5.98	−6.31	−5.80
E_{exch}*	11.39	11.84	14.16	12.73
E_{ind}*	−1.04	−0.71	−1.33	−0.70
E_{disp}*	−11.58	−12.07	−14.26	−13.08
δ(HF)	−0.96	−0.97	−1.05	−0.99

SAPT(DFT) energy components at the optimized r_v: total interaction energy (E_{tot}), electrostatic energy (E_{es}), effective induction energy (E_{ind}*), effective dispersion energy (E_{disp}*), effective exchange repulsion energy (E_{exch}*), and delta HF correction term (δ(HF)). Here, the asterisk denotes that the induction exchange term is included in the induction energy, and the dispersion−exchange term is included in the exchange energy, while the above two terms are excluded from the exchange energy. The interaction energies for Cyt-S2, Thy-S1, Gua-S2, and Ade-S1 are 6.80, 7.89, 8.79, and 7.84 kcal/mol, respectively. Tabulated values (Table 2) include fragment relaxation energies which are unusually large in some cases, implying that MP2 geometries are incompatible with PBE0. Under estimation compared to CCSD(T)/CBS can be attributed to the incompleteness of the basis set. Overall, binding characters are similar from one another; portions of each energy component are similar throughout bases. Dispersion is the largest source of attraction, typical of dispersion-bound complexes. Owing to the molecular size, guanine and adenine surely yield larger dispersion energies than thymine and cytosine. In terms of electrostatic energy, guanine is the largest, while cytosine is the smallest.

Potential energy surface along the vertical distance gives a detailed comparison between methods. We depicted the potential energy surface of cytosine stacked on naphthalene in Figure 2. Overall, all methods are within 1 kcal/mol from the CCSD(T)/CBS limit, showing the current state-of-the-art DFT methods. These DFT methods are much faster in computation than CCSD(T)/CBS and yield reasonably satisfactory results. Most methods are underbinding, but optB86b is slightly overbinding. BLYP-D3/aVTZ is the closest to the CCSD(T)/CBS limit. However, its remarkable success should not be interpreted as a success of DFT-D3. PBE-D3/aVTZ yields binding energies lower by >1 kcal/mol than BLYP-D3 (not shown). We also remark that neglect of $1/R^8$ terms also underestimates the binding energy in BLYP-D3. The Axilrod−Teller−Muto type correction reduces the binding energy almost to the same extent regardless of the intermolecular distance. PBE + TS yields a right magnitude of the binding energy at the equilibrium point but underestimated values at short contact distances. PBE + MBD leads to a better curvature

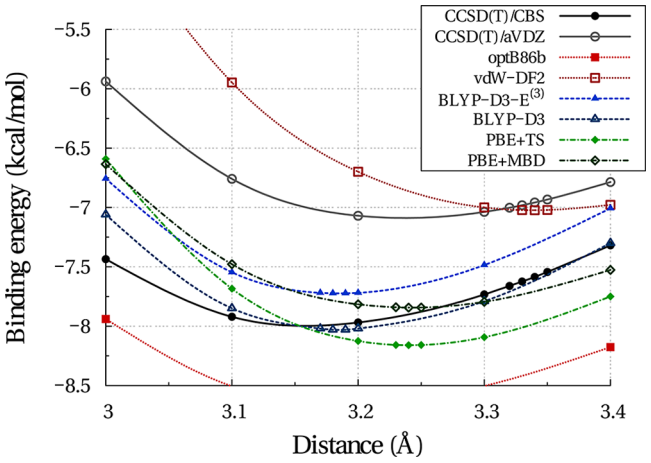

Figure 2. Total energy vs vertical distance of the cytosine−naphthalene complex from a variety of computational methods.

than PBE + TS with similar energies. In short distances, every DFT method yields a steeper curve than CCSD(T). Potential energy surface analysis reveals interesting aspects beyond test set analysis; a method, which seems to be right in test set analysis done in fixed geometries, can predict different stable geometries with different interaction energies. Benchmarks of the potential energy surface comparison type[65] is worth being encouraged.

Pairwise additive type methods outperform nonlocal correlation methods at the current stage in terms of both speed and accuracy. Although they look like an ad hoc method, they have a firm theoretical origin from ACFD correlation energy.[66] We remark that many-body screening and energy effects, beyond the standard pairwise approximation to vdW interactions, are known to considerably affect the binding of molecules with large aromatic compounds.[22,61] (A 'body' means an atom in this context.) We expect these many-body effects to also play an important role for the binding of DNA molecules to graphene. Work is ongoing to assess the role of many-body interactions for adsorption of molecules on graphitic materials.

We investigate extended systems as well. Traditional quantum chemical methods, such as MP2 and CCSD, are too expensive, if not impossible, to be applied to extended structure like graphene. Therefore, we adopt two DFT methods used above (Table 4). We carry out the geometry optimization of a

Table 4. Binding Energies (kcal/mol) and Vertical Distances (Å) (in parentheses) for the Lowest-Energy Stacked Configurations between a Nucleobase and Graphene

$E_b(r_v)$	Cyt	Thy	Gua	Ade
optB86b	18.0(3.15)	19.2(3.18)	22.3(3.17)	19.9(3.26)
PBE + TS	18.4(3.23)	19.7(3.23)	21.7(3.27)	19.8(3.27)

nucleobase with periodic boundary conditions while fixing the unit cell and the graphene sheet (Figure 3). Table 3 shows binding energies and vertical distances. For optB86b, the binding energy follows the same trend as when naphthalene is attached. For PBE + TS, adenine and thymine bind with almost the same stabilization. This behavior is consistent with the study by Antony et al.[41] The magnitude of binding energy is almost doubled in both optB86b and TS-vdW. This is as expected because graphene offers more electrons to be involved in vdW interaction. It is likely to be overestimated because

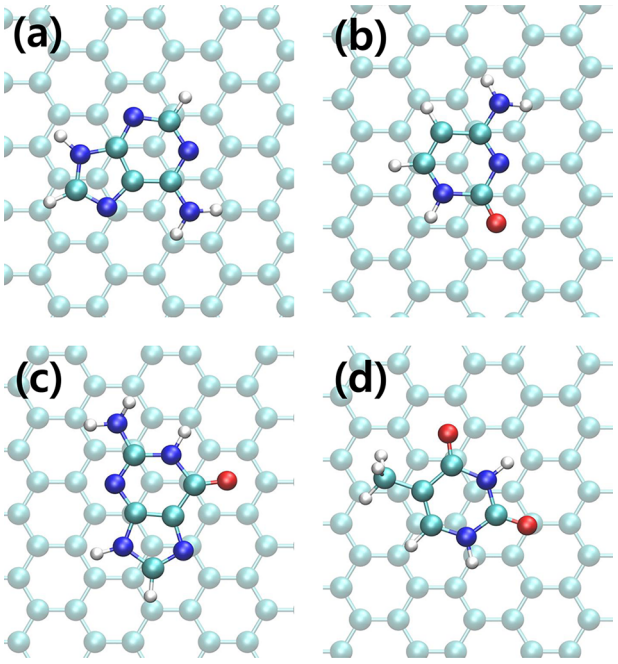

Figure 3. PBE + TS structures of graphene–nucleobase complexes: adenine (a), cytosine (b), guanine (c), and thymine (d). Green, blue, white, and red are carbon, nitrogen, hydrogen, and oxygen, respectively.

employed methods do not include screening effects. The vertical distances for the stacked geometry are 3.2–3.3 Å, similar to the naphthalene cases. However, note that B97-D shortens it to ~3.0 Å,[41] which seems to be too short due to overestimation of dispersion energy from pairwise additivity and constant C_6. The anisotropic effect for the dispersion energy correction needs to be seriously taken into account for more accurate results. Note that the most stable configuration of a nucleobase–graphene complex corresponds to Cyt-S3, Gua-S2, Thy-S2, and Ade-S2 or Ade-S4 in Figure 1. The most stable geometries are similar to those obtained by Le et al.[48] except for thymine. In our case, thymine from both PBE + TS and optB86b prefers to sit on the graphene sheet, as shown in Figure 3.

We have also studied nucleobase–graphene flake complexes. The three flakes of hexagonal symmetry are made up of 54 carbons and 18 hydrogens on edges for n = 3, 96 carbons and 24 hydrogens on edges for n = 4, and 150 carbons and 30 hydrogens on edges for n = 5. Every geometry is fully optimized at the PBE + TS/tier 2 level (tight setting) with FHI-AIMS. Therefore, relaxation energies of a flake and a nucleobase are fully taken into account. D3 calculations are done at the same geometry as PBE + TS. The result does not suffer from spurious multipole interactions between unit cells. The above two are the main reasons to compute flakes. The flakes become very slightly concave as a nucleobase is physisorbed (see Figure 4 for n = 5). We plot binding energies against $1/N^2$, where N is the number of carbon atoms in the flake (Figure 5). Note that the three points give almost a straight line for this fitting. A result for n = 5 is already close to the corresponding extrapolated value. However, as we stressed, the convergence does not include the long-range screening effects which are expected to be significant in these systems. It merely manifests that carbon atoms too close to (or far from) a base substantially (or barely) contribute to binding in terms of dispersion. Adding

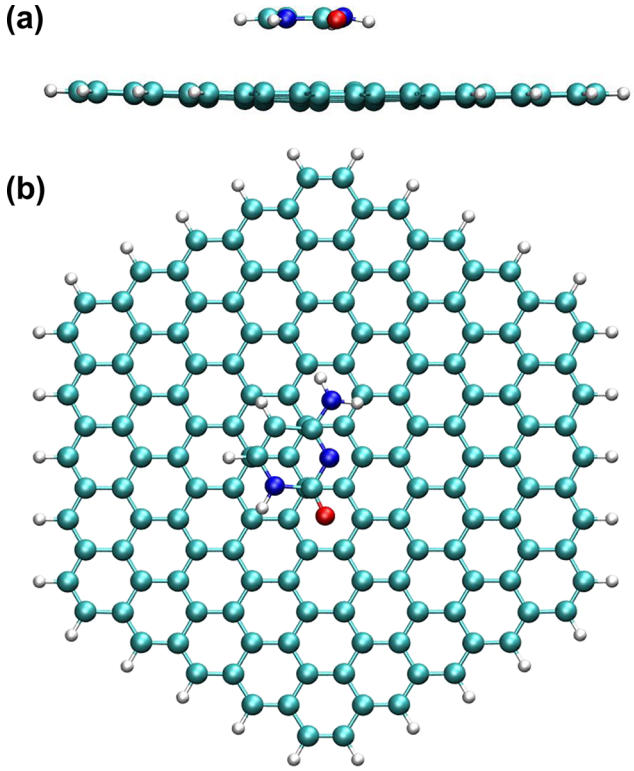

Figure 4. The geometry of a cytosine–graphene flake (n = 5) complex. (a) A graphene flake becomes slightly concave when bound to a nucleobase, manifested from a side view. (b) A top view shows that the binding geometry is similar to the case when the periodic boundary condition is used.

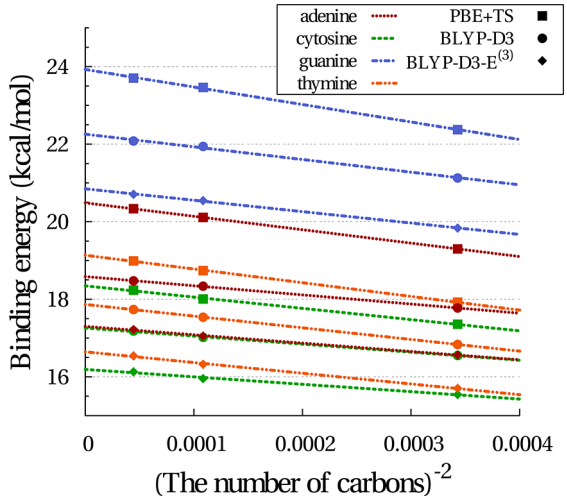

Figure 5. Binding energies with increasing flake sizes to obtain the extrapolated values for the infinite sizes. The binding energies are plotted against $1/N^2$, where N is the number of carbon atoms in the flake.

three-body terms does not change the behavior. It reduces the binding energy by a constant as in the case of naphthalene. Overall, the binding energies are similar to those obtained using the periodic boundary cases in that the trend is identical. The geometry is also very similar to the periodic boundary case; except for slight concaveness, a nucleobase prefers the same configuration on a flake as on a periodic graphene sheet. The relaxation energy of the graphene flake n = 5 is ~0.4 kcal/mol

dx.doi.org/10.1021/ct301097u | J. Chem. Theory Comput. 2013, 9, 2090–2096

on average, with deviations from one base to another <0.1 kcal/mol.

4. CONCLUDING REMARKS

We studied the binding energy and distance of nucleobase on naphthalene and graphene. We applied SCS-MP2, CCSD(T), and SAPT as well as DFT methods such as Grimme's, Dion's nonlocal, and TS functionals. The CCSD(T)/CBS binding energies of cytosine, thymine, guanine, and adenine on naphthalene are 7−9 kcal/mol. As we applied the DFT methods (PBE+TS/tier2) to the extended systems where the nucleobase sits on graphene, their binding energy on graphene is 18−24 kcal/mol. Their binding energies of nucleobases on graphene are found to be large enough to stabilize nucleobases on the graphene sheet. However, doubling of binding energies from naphthalene to graphene needs more investigations since the many-body effects on screening and on energy are known to play a role in this type of system. In this regard, the issue of the binding of nucleobases on graphene has not been fully resolved.

AUTHOR INFORMATION

Corresponding Author

*E-mail: kim@postech.ac.kr

Present Address

[‖]Max-Planck Institut für Mikrostrukturphysik, Weinberg 2, D-06120 Halle, Germany

Notes

The authors declare no competing financial interest.

ACKNOWLEDGMENTS

This work was supported by NRF (National Honor Scientist Program: 2010-0020414, WCU: R32-2008-000-10180-0) and KISTI (KSC-2011-G3-02).

REFERENCES

(1) Kim, K. S.; Tarakeshwar, P.; Lee, J. Y. *Chem. Rev.* **2000**, *100*, 4145.
(2) Hobza, P.; Selzle, H. L.; Schlag, E. W. *Chem. Rev.* **1994**, *94*, 1767.
(3) Hunter, C. A.; Sanders, J. K. M. *J. Am. Chem. Soc.* **1990**, *112*, 5525.
(4) Hoeben, F. J. M.; Jonkheijm, P.; Meijer, E. W.; Schenning, A. P. H. J. *Chem. Rev.* **2005**, *105*, 1491.
(5) Lee, J. Y.; Hong, B. H.; Kim, W. Y.; Min, S. K.; Kim, Y.; Jouravlev, M. V.; Bose, R.; Kim, K. S.; Hwang, I.-C.; Kaufman, L. J.; Wong, C. W.; Kim, P.; Kim, K. S. *Nature* **2009**, *460*, 498.
(6) Meyer, E. A.; Castellano, R. K.; Diederich, F. *Angew. Chem., Int. Ed.* **2003**, *42*, 1210.
(7) Che, Y.; Datar, A.; Balakrishnan, K.; Zang, L. *J. Am. Chem. Soc.* **2007**, *129*, 7234.
(8) Hong, B. H.; Bae, S. C.; Lee, C.-W.; Jeong, S.; Kim, K. S. *Science* **2001**, *294*, 348.
(9) Sessler, J. L.; Lawrence, C. M.; Jayawickramarajah, J. *Chem. Soc. Rev.* **2007**, *36*, 314.
(10) Ma, J. C.; Dougherty, D. A. *Chem. Rev.* **1997**, *97*, 1303.
(11) Podeszwa, R.; Bukowski, R.; Szalewicz, K. *J. Phys. Chem. A* **2006**, *110*, 10345.
(12) Singh, N. J.; Min, S. K.; Kim, D. Y.; Kim, K. S. *J. Chem. Theory Comput.* **2009**, *5*, 515.
(13) Tarakeshwar, P.; Choi, H. S.; Kim, K. S. *J. Am. Chem. Soc.* **2001**, *123*, 3323.
(14) Lee, E. C.; Hong, B. H.; Lee, J. Y.; Kim, J. C.; Kim, D.; Kim, Y.; Tarakeshwar, P.; Kim, K. S. *J. Am. Chem. Soc.* **2005**, *127*, 4530.
(15) Bloom, J. W. G.; Raju, R. K.; Wheeler, S. E. *J. Chem. Theory Comput.* **2012**, *8*, 3167.
(16) Pitoňák, M.; Neogrády, P.; Řezáč, J.; Jurečka, P.; Urban, M.; Hobza, P. *J. Chem. Theory Comput.* **2008**, *4*, 1829.
(17) Lee, E. C.; Kim, D.; Jurečka, P.; Tarakeshwar, P.; Hobza, P.; Kim, K. S. *J. Phys. Chem. A* **2007**, *111*, 3446.
(18) Sinnokrot, M. O.; Sherrill, C. D. *J. Phys. Chem. A* **2006**, *110*, 10656.
(19) Sinnokrot, M. O.; Sherrill, C. D. *J. Phys. Chem. A* **2004**, *108*, 10200.
(20) Ringer, A. L.; Sinnokrot, M. O.; Lively, R. P.; Sherrill, C. D. *Chem.—Eur. J.* **2006**, *12*, 3821.
(21) Tsuzuki, S.; Honda, K.; Uchimaru, T.; Mikami, M. *J. Chem. Phys.* **2006**, *125*, 124304.
(22) Tkatchenko, A.; Alfè, D.; Kim, K. S. *J. Chem. Theory Comput.* **2012**, *8*, 4317.
(23) Antony, J.; Grimme, S. *J. Phys. Chem. A* **2007**, *111*, 4862.
(24) Piacenza, M.; Grimme, S. *J. Am. Chem. Soc.* **2005**, *127*, 14841.
(25) Jurečka, P.; Hobza, P. *J. Am. Chem. Soc.* **2003**, *125*, 15608.
(26) Jurečka, P.; Šponer, J.; Černý, J.; Hobza, P. *Phys. Chem. Chem. Phys.* **2006**, *8*, 1985.
(27) Šponer, J.; Riley, K. E.; Hobza, P. *Phys. Chem. Chem. Phys.* **2008**, *10*, 2595.
(28) Geim, A. K. *Science* **2009**, *324*, 1530.
(29) Kim, K. S.; Zhao, Y.; Jang, H.; Lee, S. Y.; Kim, J. M.; Kim, K. S.; Ahn, J.-H.; Kim, P.; Choi, J.-Y.; Hong, B. H. *Nature* **2009**, *457*, 706.
(30) Schwierz, F. *Nat. Nanotechnol.* **2010**, *5*, 487.
(31) Kim, W. Y.; Kim, K. S. *Nat. Nanotechnol.* **2008**, *3*, 408.
(32) Park, J.; Lee, W. H.; Huh, S.; Sim, S. H.; Kim, S. B.; Cho, K.; Hong, B. H.; Kim, K. S. *J. Phys. Chem. Lett.* **2011**, *2*, 841.
(33) Williams, J. R.; Low, T.; Lundstrom, M. S.; Marcus, C. M. *Nat. Nanotechnol.* **2011**, *6*, 222.
(34) Chandra, V.; Park, J.; Chun, Y.; Lee, J. W.; Hwang, I.-C.; Kim, K. S. *ACS Nano* **2010**, *4*, 3979.
(35) Du, X.; Skachko, I.; Barker, A.; Andrei, E. Y. *Nat. Nanotechnol.* **2008**, *3*, 491.
(36) Sun, Y.; Wu, Q.; Shi, G. *Energy Environ. Sci.* **2011**, *4*, 1113.
(37) Georgakilas, V.; Otyepka, M.; Bourlinos, A. B.; Chandra, V.; Kim, N.; Kemp, K. C.; Hobza, P.; Zboril, R.; Kim, K. S. *Chem. Rev.* **2012**, *112*, 6156.
(38) Min, S. K.; Kim, W. Y.; Cho, Y.; Kim, K. S. *Nat. Nanotechnol.* **2011**, *6*, 162.
(39) Min, S. K.; Cho, Y.; Mason, D. R.; Lee, J. Y.; Kim, K. S. *J. Phys. Chem. C* **2011**, *115*, 16247.
(40) Gowtham, S.; Scheicher, R. H.; Ahuja, R.; Pandey, R.; Karna, S. P. *Phys. Rev. B* **2007**, *76*, 033401.
(41) Antony, J.; Grimme, S. *Phys. Chem. Chem. Phys.* **2008**, *10*, 4862.
(42) Berland, K.; Chakarova-Käck, S. D.; Cooper, V. R.; Langreth, D. C.; Schröder, E. *J. Phys.: Condens. Matter* **2011**, *23*, 135001.
(43) Dion, M.; Rydberg, H.; Schröder, E.; Langreth, D. C.; Lundqvist, B. I. *Phys. Rev. Lett.* **2004**, *92*, 246401.
(44) Le, D.; Kara, A.; Schröder, E.; Hyldgaard, P.; Rahman, T. S. *J. Phys.: Condens. Matter* **2012**, *24*, 424210.
(45) Spiwok, V.; Hobza, P.; Řezáč, J. *J. Phys. Chem. C* **2011**, *115*, 19455.
(46) Misquitta, A. J.; Podeszwa, R.; Jeziorski, B.; Szalewicz, K. *J. Chem. Phys.* **2005**, *123*, 214103.
(47) Klimeš, J.; Bowler, D. R.; Michaelides, A. *Phys. Rev. B* **2011**, *83*, 195131.
(48) Lee, K.; Murray, É. D.; Kong, L.; Lundqvist, B. I.; Langreth, D. C. *Phys. Rev. B* **2010**, *82*, 081101.
(49) Tkatchenko, A.; Scheffler, M. *Phys. Rev. Lett.* **2009**, *102*, 073005.
(50) Elstner, M.; Hobza, P.; Frauenheim, T.; Suhai, S.; Kaxiras, E. *J. Chem. Phys.* **2001**, *114*, 5149.
(51) Min, S. K.; Lee, E. C.; Lee, H. M.; Kim, D. Y.; Kim, D.; Kim, K. S. *J. Comput. Chem.* **2008**, *29*, 1208.
(52) Sinnokrot, M. O.; Valeev, E. F.; Sherrill, C. D. *J. Am. Chem. Soc.* **2002**, *124*, 10887.
(53) Werner, H. J.; Knowles, P. J.; Knizia, G.; Manby, F. R.; Schütz, M.; Celani, P.; Korona, T.; Lindh, R.; Mitrushenkov, A.; Rauhut, G.; Shamasundar, K. R.; Adler, T. B.; Amos, R. D.; Bernhardsson, A.;

Berning, A.; Cooper, D. L.; Deegan, M. J. O.; Dobbyn, A. J.; Eckert, F.; Goll, E.; Hampel, C.; Hesselmann, A.; Hetzer, G.; Hrenar, T.; Jansen, G.; Köppl, C.; Liu, Y.; Lloyd, A. W.; Mata, R. A.; May, A. J.; McNicholas, S. J.; Meyer, W.; Mura, M. E.; Nicklass, A.; O'Neill, D. P.; Palmieri, P.; Pflüger, K.; Pitzer, R.; Reiher, M.; Shiozaki, T.; Stoll, H.; Stone, A. J.; Tarroni, R.; Thorsteinsson, T.; Wang, M.; Wolf, A.*MOLPRO a package of ab initio programs molpro*, version 2010.1; University College Cardiff Consultants Limited: Cardiff, U.K., 2010.
(54) Grimme, S. *J. Chem. Phys.* **2003**, *118*, 9095.
(55) Grüning, M.; Gritsenko, O. V.; van Gisbergen, S. J. A.; Baerends, E. J. *J. Chem. Phys.* **2001**, *114*, 652.
(56) Adamo, C.; Barone, V. *J. Chem. Phys.* **1999**, *110*, 6158.
(57) Grimme, S.; Antony, J.; Ehrlich, S.; Krieg, H. *J. Chem. Phys.* **2010**, *132*, 154104.
(58) Kresse, G.; Furthmüller, J. *Phys. Rev. B* **1996**, *54*, 11169.
(59) Román-Pérez, G.; Soler, J. M. *Phys. Rev. Lett.* **2009**, *103*, 096102.
(60) Blum, V.; Gehrke, R.; Hanke, F.; Havu, P.; Havu, V.; Ren, X.; Reuter, K.; Scheffler, M. *Comput. Phys. Commun.* **2009**, *180*, 2175.
(61) Tkatchenko, A.; DiStasio, R. A.; Car, R.; Scheffler, M. *Phys. Rev. Lett.* **2012**, *108*, 236402.
(62) Bachorz, R. A.; Bischoff, F. A.; Glöß, A.; Hättig, C.; Höfener, S.; Klopper, W.; Tew, D. P. *J. Comput. Chem.* **2011**, *32*, 2492.
(63) Hättig, C.; Tew, D. P.; Köhn, A. *J. Chem. Phys.* **2010**, *132*, 231102.
(64) Marshall, M. S.; Sherrill, C. D. *J. Chem. Theory Comput.* **2011**, *7*, 3978.
(65) Podeszwa, R.; Szalewicz, K. *J. Chem. Phys.* **2012**, *136*, 161102.
(66) Tkatchenko, A.; Ambrosetti, A.; DiStasio, J. R. A. *J. Chem. Phys.* **2013**, *138*, 074106.